Journal of Computational Physics **172,** 198–208 (2001)
doi:10.1006/jcph.2001.6820, available online at http://www.idealibrary.com on IDEAL®

Adaptive Mesh Enrichment for the Poisson–Boltzmann Equation

Pavel Dyshlovenko

Department of Physics, Ul'yanovsk State Technical University, 32 Severny Venets Street, Ul'yanovsk 432027, Russia
E-mail: pavel@ulstu.ru

Received March 17, 2000; revised September 21, 2000

An adaptive mesh enrichment procedure for a finite-element solution of the two-dimensional Poisson–Boltzmann equation is described. The mesh adaptation is performed by subdividing the cells using information obtained in the previous step of the solution and next rearranging the mesh to be a Delaunay triangulation. The procedure allows the gradual improvement of the quality of the solution and adjustment of the geometry of the problem. The performance of the proposed approach is illustrated by applying it to the problem of two identical colloidal particles in a symmetric electrolyte. © 2001 Academic Press

Key Words: adaptive mesh refinement; mesh enrichment; Delaunay triangulation; finite-element method; Poisson–Boltzmann equation; colloidal particles interaction.

1. INTRODUCTION

The nonlinear Poisson–Boltzmann (PB) equation is used for the description of the distribution of electrostatic potential in colloidal dispersions [1, 2]. Knowing the electrostatic potential, one can calculate other quantities such as the free energy of a colloidal system and the resulting force of particle–particle interaction. Features of interparticle interaction are of great importance for the stability and properties of colloidal dispersions. One of the most intriguing phenomena is metastable superheated crystalline structures performed by identical charged latex spheres in water [3]. The structure and dynamics of these metastable colloidal crystals seem to be accounted for by the long-range attraction between the similarly charged spherical particles. Numerical investigation of models based on the PB equation can provide important information on effective interparticle interaction in colloidal systems.

An approach based on the PB equation can be applied to the analysis of the well known problem of two identical charged spherical particles immersed in a symmetric univalent electrolyte. Owing to the geometrical symmetry, it can be reduced to two dimensions and is very suitable for the testing of different numerical methods. The problem of interaction of two

0021-9991/01 $35.00
Copyright © 2001 by Academic Press
All rights of reproduction in any form reserved.

identical colloidal particles was studied numerically by finite-difference methods in [4–6] and by finite-element methods in [7–9]. The application of finite-difference methods is based mainly on the introduction of a bispherical coordinate system, which is very convenient in the given special problem. Bispherical coordinates allow the use of regular grids in the domain of the problem which is important for finite-difference methods. A fourth-order discretization based on collocation with bi-cubic Hermite basis functions together with a regular grid in the domain of bispherical coordinates was also used in [8] and produces highly accurate results.

In the present paper the finite-element method with adaptive mesh enrichment is described. Error analysis permits determination of those cells that have a high level of error and hence should be subdivided. The marked cells are subdivided and the computations are carried out again on the new mesh. The process is repeated until the desired level of accuracy is reached. The boundaries of the solution domain are also subdivided automatically to satisfy the prescribed solution quality. The mesh is a Delaunay triangulation (DT) in each step of the solution which allows triangular cells to be as perfect as possible for a given set of the nodes. The method is flexible enough to solve the problems in which the regions of high gradient, and hence high errors, of the potential are not known a priori: these regions are detected automatically. The performance of the proposed approach is demonstrated by using it to solve the test problem of two interacting identical colloidal particles. However the method can be adjusted for two-dimensional problems with more sophisticated geometry including both rectilinear and curvilinear boundaries.

Using irregular meshes and the adaptive technique to solve the PB equation for the problem of interaction of colloidal particles has previously been done in [9]. The Galerkin finite-element method with nine-noded quadrilateral elements combined with an adaptive remeshing was employed. The final mesh was optimal in the sense that each element in the mesh has nearly the same value of error. The power of the method was demonstrated by two different examples: two interacting identical spherical particles, and a single spherical particle at various distances to a cylindrical pore in a planar surface. In both cases, the method allowed construction of effective meshes and produced final results with a prescribed accuracy of less than 1%.

The distinctive features of the approach of the present paper are the following. First, six-noded triangular elements are employed which allow the use of the DT process for improving the quality of the mesh. Then, the enrichment technique combined with DT rearranging is used instead of remeshing. The enrichment process involves subdivision of elements of a current mesh while remeshing means completely regenerating the mesh in each step of the solution. Enrichment in conjunction with DT can also be a successful mesh adaptation technique for the PB equation. The initial mesh is not quasi-uniform but has a variable density depending on the expected initial error distribution within the domain (see Section 3.5). In addition, final numerical results, at least for F_m (see Section 4), are probably more accurate.

2. DESCRIPTION OF THE PROBLEM

The proposed approach is demonstrated by solving the PB equation for the system of two identical spherical colloidal particles in a symmetric univalent electrolyte. The case of constant surface potential [8] is considered. The geometry of the problem is shown in Fig. 1.

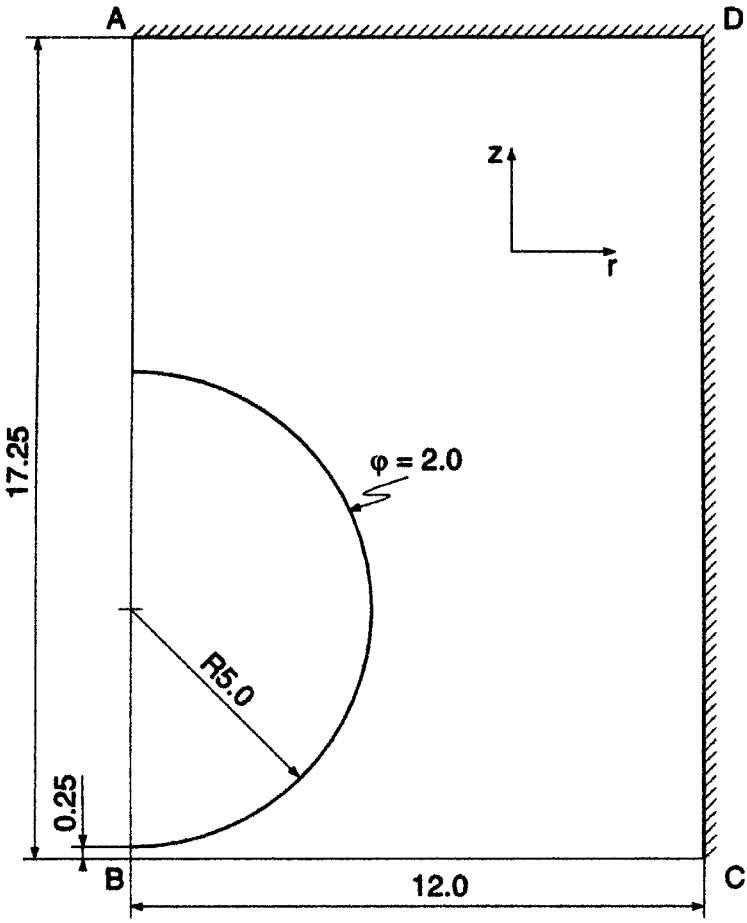

FIG. 1. The domain for the problem of two interacting identical spherical particles. AB is the axis of rotational symmetry; BC represents the median plane; ADC designates the walls of a cylindrical vessel.

The dimensionless PB equation for electrostatic potential ϕ outside the spheres in cylindrical coordinates takes the form

$$\frac{\partial^2\phi}{\partial r^2} + \frac{1}{r}\frac{\partial\phi}{\partial r} + \frac{\partial^2\phi}{\partial z^2} = \sinh\phi. \tag{1}$$

Length, electrostatic potential, and force are respectively measured in units of Debye length $\kappa^{-1} = (2nq_e^2/\epsilon kT)^{-1/2}$, kT/q_e, and $\epsilon(kT/q_e)^2$, where n is the concentration of any of the species in the electrolyte, q_e is the absolute value of electronic charge, ϵ is the absolute permittivity of the electrolyte, k is the Boltzmann constant, T is the absolute temperature, and the rationalised SI is used to express the factors.

The dimensionless electrostatic potential of the surfaces of either particle is chosen to be 2.0 and is kept constant. The Neumann boundary conditions $\partial\phi/\partial\mathbf{n} = 0$ are implied on the other boundaries of the domain. Electric fields inside the particles are absent.

The electric field is related to the potential by the equation

$$\mathbf{E} = -\nabla\phi. \tag{2}$$

The force of interaction of the particles is obtained by means of direct integration of the total stress tensor over the appropriate surface [10]. There are at least two possible ways of integrating: over the surface of the particle and over the median plane [7, 9]. The dimensionless force obtained by integrating over the surface of the particle is calculated according to the expression

$$F_s = \frac{1}{2} \int\limits_{\substack{\text{Surface} \\ \text{of the particle}}} \left(E_r^2 + E_z^2\right) \mathbf{n} \cdot \mathbf{e}_z \, da, \tag{3}$$

where $\mathbf{n}$ is the outward unit norm vector of the surface element, and $\mathbf{e}_z$ is the unit vector in the z-direction. For the integration over the median plane, the dimensionless force is

$$F_m = \frac{1}{2} \int\limits_{\text{Midplane}} \left[2(\cosh\phi - 1) + E_r^2\right] \, da. \tag{4}$$

The latter case is more accurate since different pieces of the midplane contribute with the same sign. In both expressions the vector of electric field $\mathbf{E}$ is assumed to be perpendicular to the corresponding surfaces which is actually approximately valid due to the numerical errors.

3. ADAPTIVE PROCESS

The solution of the PB equation with adaptive mesh refinement is a cyclic process. Starting from the initial mesh, it passes repeatedly through the following steps:

1. Numerical solution of the equation on a given mesh, the mesh being a DT.
2. Evaluation of both the global error and errors in each element of the mesh.

The global error of the solution is assumed to get smaller as the process revolves. If the desired accuracy is reached, the process stops. If not, a decision is made for each cell on whether a particular cell should be subdivided or not. The decision is based upon the values of individual errors of the elements.

3. Subdivision of marked cells. The mesh loses its property to be a DT in general.
4. Modification of the mesh to become a DT. Computation can proceed again on the new mesh.

The process is repeated until the desired accuracy level is reached (in step 2). The steps of the adaptive process are considered below in further detail.

3.1. *Numerical Solution*

In the present paper the PB equation was solved by the Galerkin method [11] on the mesh of six-noded triangular elements. The system of nonlinear equations resulting from the discretisation process was solved using the quasi-Newton approach [12]. Once the finite-element (FE) solution for electrostatic potential ϕ has been obtained, the components of electric field vector $\mathbf{E}$ are calculated by direct differentiation of this solution with respect to the corresponding coordinates according to Eq. (2). This kind of solution for $\mathbf{E}$ is also called the FE solution and will be designated $\hat{\mathbf{E}}$. The components of $\hat{\mathbf{E}}$ are discontinuous

across the boundaries of the elements. The details of the numerical procedures [13] are rather standard and are not discussed in the present paper.

3.2. *Error Evaluation*

An a posteriori error estimator of the type proposed by Zienkiewicz and Zhu [14] is used for estimating the error of the solution. The FE solution $\hat{\mathbf{E}}$ for the electric field, which is, to within a sign, a gradient of electrostatic potential, is compared with an alternative postprocessed recovered solution. The latter is often called the "exact" solution and will be designated $\tilde{\mathbf{E}}$. To obtain $\tilde{\mathbf{E}}$, various gradient recovery techniques can be employed. In the present paper, a very simple gradient recovery procedure based on averaging the nodal values of the FE solution $\hat{\mathbf{E}}$ is used. The components of $\tilde{\mathbf{E}}$ are expressed via the same basic functions that were used for the electrostatic potential and are continuous.

In the case of the exact solution variables $\hat{\mathbf{E}}$ and $\tilde{\mathbf{E}}$ must coincide. In general, the error is defined as a deviation of one variable from the other. More precisely, the global absolute error δ is defined by the expression

$$\delta = \left\{ \int_{\Omega} [(\hat{E}_r - \tilde{E}_r)^2 + (\hat{E}_z - \tilde{E}_z)^2]\, dr\, dz \right\}^{1/2}, \tag{5}$$

the integral being taken over the whole domain Ω. This is simply a L^2-norm of the difference $\hat{\mathbf{E}} - \tilde{\mathbf{E}}$. The global relative error ϵ is defined by

$$\epsilon = \frac{\delta}{\|\hat{\mathbf{E}}\|}, \tag{6}$$

where

$$\|\hat{\mathbf{E}}\| = \left\{ \int_{\Omega} \left(\hat{E}_r^2 + \hat{E}_z^2\right) dr\, dz \right\}^{1/2}. \tag{7}$$

Absolute error δ_i in a particular element i is defined as in Eq. (5) except that the integral is taken over the element. The relation

$$\delta^2 = \sum_{i=1}^{N} \delta_i^2 \tag{8}$$

must hold, where N is the total number of elements in the mesh.

The level of accuracy is determined by the prescribed global relative error ϵ_{pre} and the corresponding absolute error $\delta_{pre} = \epsilon_{pre}\|\hat{\mathbf{E}}\|$. Given δ_{pre}, the current mean absolute error δ_m in an element can be calculated according to

$$\delta_m = \left[\frac{\delta_{pre}^2}{N}\right]^{1/2} = \left[\frac{(\epsilon_{pre}\|\hat{\mathbf{E}}\|)^2}{N}\right]^{1/2}. \tag{9}$$

The current number of elements would each have to have this value of absolute error to provide the prescribed level of accuracy, on the condition that absolute errors in all the

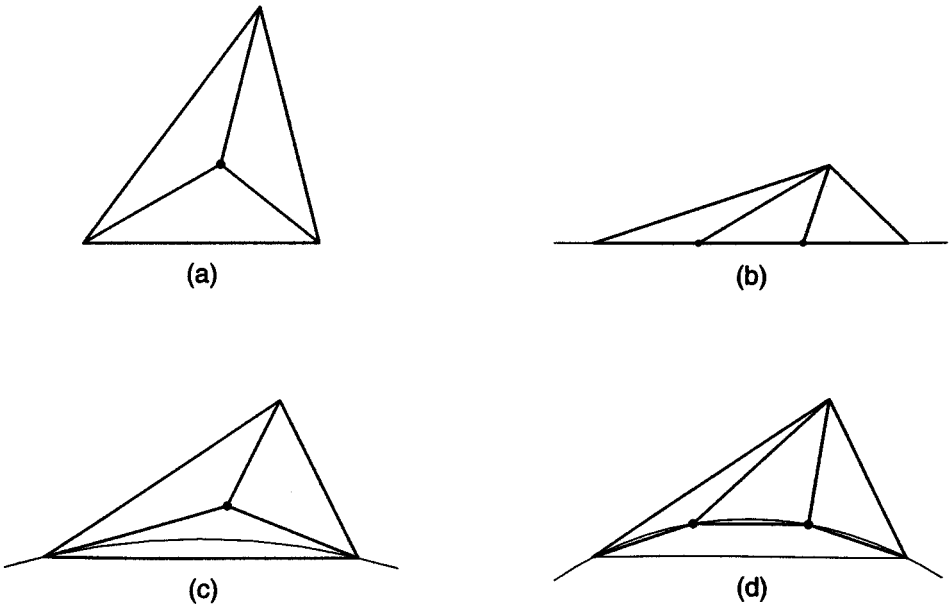

FIG. 2. Subdivision of cells (see Section 3.3): (a) Internal cell and cell adjoining a rectilinear boundary. (b) Stretched cell adjoining a rectilinear boundary. (c) Cell adjoining a circular boundary of small curvature. (d) Cell adjoining a circular boundary of large curvature.

elements were the same. Those elements whose absolute errors exceed the current mean absolute error δ_m are chosen to be subjected to subdivision.

3.3. *Subdivision of Cells*

A triangular cell is called internal if none of its sides belongs to the boundary of the problem's domain.

1. If a cell is internal, a new node is placed at the barycentre of the triangle and connected to the vertices of the cell. Three new triangles appear instead of the former triangle (see Fig. 2a).

If a cell is not internal, at least one of its sides belongs to the boundary of the domain. Two different situations are considered: rectilinear boundary and circular boundary.

If a cell adjoins the rectilinear boundary it is divided in either of the following ways.

2a. If the circumcentre of the triangle is located within the domain, a new node is placed at the barycentre of the triangle as for an internal cell.

2b. If the circumcentre of the triangle is beyond the domain, an alternative method is used. Two new nodes are placed on the corresponding boundary side dividing it into three equal parts. Then the new nodes are connected to the opposite vertex of the cell and three new triangles appear instead of the former triangle (see Fig. 2b).

The circular boundary is actually represented by a broken line. There should be enough segments in the broken line for an efficient reproduction of the shape of the curvilinear boundary and for sufficiently high accuracy of the solution. The number of segments can be increased during the calculations.

If a cell adjoins the circular boundary, it is divided in one of the following ways.

3a. If the circumcentre of the triangle is located within the domain, a new node is placed at the barycentre of the triangle on the condition that the sides of the new triangles do not cross the imaginary circular boundary (see Fig. 2c).

3b. If the circumcentre of the triangle is located within the domain and division according to point 3a is impossible, an alternative method is used. The boundary side of the cell that corresponds to the circular boundary is divided into three equal parts by means of two new nodes. Then the new nodes are shifted along the radii of the circle to be allocated on the circumference and connected to the vertices of the cell, thus producing three new triangles (see Fig. 2d).

3c. If the circumcentre of the triangle is beyond the domain, the method of point 3b is always used.

The proposed algorithm provides efficient adaptive division of both the interior and the boundaries of the domain.

3.4. *Delaunay Triangulation*

Meshes employed in the problem are Delaunay triangulation (DT) of the domain [15]. DT provides locally the "most perfect" triangles. More precisely, let the pair of triangles have a side in common. The common side can be thrown over between the vertices of the triangles to make a new pair of triangles instead of the former one (see Fig. 3). Such a transfer is called a flip. A particular mesh is DT if and only if the minimal angle of the six angles in any pair of adjacent triangles is not magnified by a flip.

The property of DT to produce "perfect" triangles is equivalent to the so-called circular criterion: mesh is DT if and only if the circumscribed circle of each triangle does not contain any other node of the mesh.

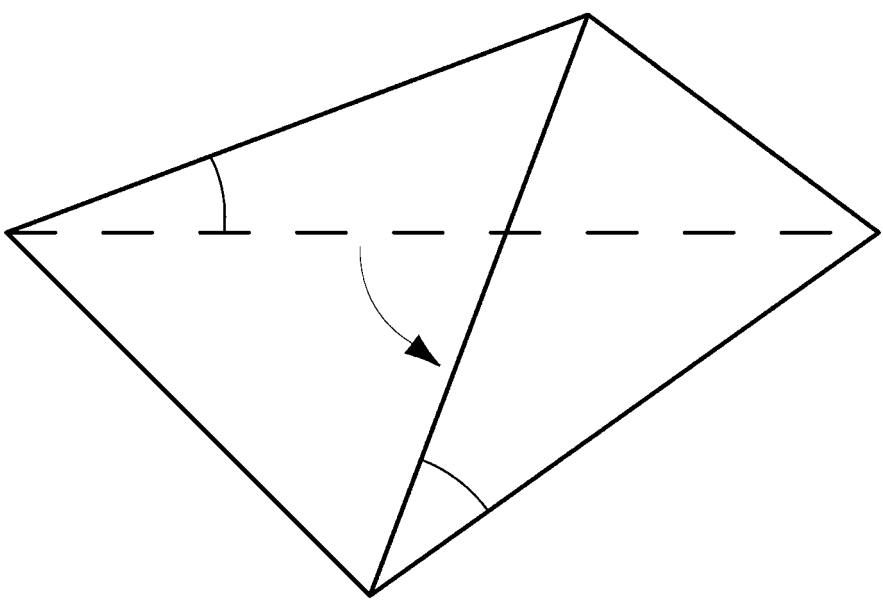

FIG. 3. Flip of the common side of two neighbour triangles.

The division of cells perturbs the mesh which is in general no longer DT. An algorithm based on the circular criterion has been implemented to convert the mesh perturbed by the division process back to DT. Each of the newly obtained triangles is checked in turn as to whether it satisfies the circular criterion. If not, the corresponding flip is performed and each of the triangles resulting from the flip is checked again, and so on. This recursive procedure usually generates few flips, if any at all. However, it can sometimes cause a long sequence of flips and affects a significant part of the domain.

After the recursive procedure has been applied to each triangle produced by the division process, the mesh will be DT.

3.5. *Initial Mesh*

An initial mesh of sufficient quality is needed to launch the adaptive numerical process. Creation of an initial mesh starts from constructing by hand a coarse germ grid of triangular elements which completely covers the solution domain. The purpose of the germ grid is to resolve the domain with rectilinear and circular boundaries into a number of triangles of reasonable shape, the number possibly being very small. The germ grid for the problem of interaction of two identical colloidal particles is shown in Fig. 4a.

Once the germ grid has been created, the subdivision process discussed above is applied to generate an initial mesh. The only distinction is that different criteria for whether a cell should be subdivided are invoked rather than the criterion described at the end of Section 3.2.

The first approach is based on a simple indicator of type $\exp(-r)$, where r is the shortest distance from the barycentre of a triangular cell to the boundary at constant nonzero potential, for instance, to the surface of the particle. The elements with indicators greater than some preset level are subdivided. The expression $\exp(-r)$ can be treated as a very rough approximation of the distribution of electrostatic potential in a real problem. Nevertheless, it works quite well for an initial mesh generation. This approach induces the most refining in those areas of the domain where the gradient of the solution is expected to be high.

Another approach is a forced subdivision of cells adjoining certain boundaries. In particular, it allows the desired initial geometrical representation of a circular boundary by a

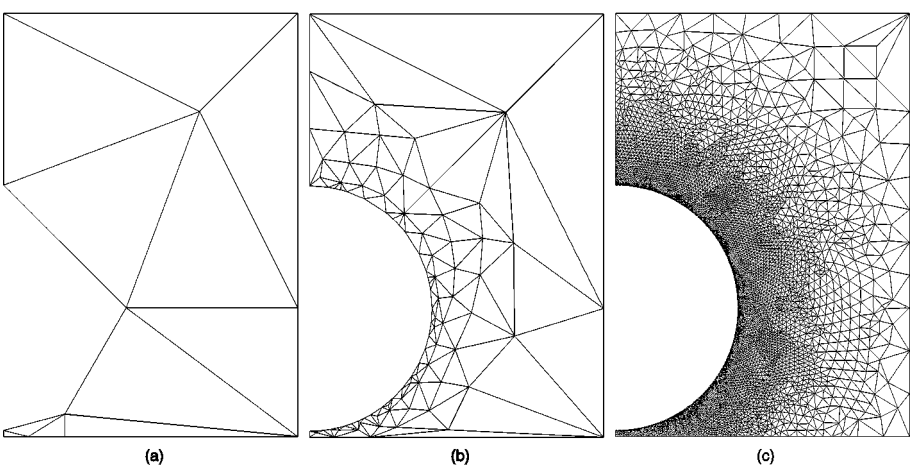

FIG. 4. Meshes for the problem of interaction of two identical spherical particles: (a) germ mesh, 11 cells, (b) initial mesh, 147 cells, (c) final mesh (after 8 steps), 16625 cells.

TABLE I
Steps of the Adaptive Process

Step number	Global relative error ϵ (%)	Force of interaction		Number of segments[a]	Length of the biggest segment[a]
		F_s	F_m		
1	4.8994	8.997	15.384	33	1.054
2	1.5148	13.608	15.517	53	1.054
3	0.5076	14.322	15.529	87	0.368
4	0.1942	14.933	15.541	173	0.256
5	0.0831	15.313	15.543	263	0.123
6	0.0397	15.438	15.544	505	0.085
7	0.0275	15.504	15.545	699	0.041
8	0.0233	15.574	15.545	961	0.033

[a] The segments of the broken line representing the circular boundary.

broken line. Then, the boundary can be additionally subdivided during the adaptive process depending on the accuracy of the solution.

Combining these two methods, one can generate an initial mesh of quality sufficient to obtain a reasonable initial numerical solution on it. The initial mesh for the problem studied in the present paper is shown in Fig. 4b.

4. RESULTS AND DISCUSSION

The germ, initial, and final meshes for the problem studied in the present paper are shown in Fig. 4. Some details of the solution at each step of the adaptive process are brought together in Table I.

The second column of the table contains the current global relative error ϵ which is defined by Eq. (6). The third and fourth columns of Table I contain numerical results for the forces of interaction F_s and F_m. The forces are calculated according to Eq. (3) and Eq. (4), respectively, the FE solution $\hat{\mathbf{E}}$ for the electric field being used. The use of the recovered solution $\tilde{\mathbf{E}}$ does not contribute significantly to increasing the accuracy compared with $\hat{\mathbf{E}}$, so corresponding results have not been included in the paper. Values of forces obtained in the present work are divided by π to unify the units. The fifth and sixth columns of Table I contain characteristics of the broken line representing the circular boundary.

The numerical results for the force of interaction are compared with the previous results in Table II. The data for the comparison are taken from [9]. The original sources are indicated in the table.

The global relative error ϵ in the second column of Table I decreases steadily while the process evolves. It has taken six steps to exceed the prescribed accuracy of 0.05%. Two

TABLE II
The Force of Interaction of Two Identical Colloidal Particles

Present paper		[9]		[6]	[8]
F_s	F_m	F_s	F_m	F_m	F_m
15.574	15.545	15.412	15.509	15.476	15.545

more steps raise the accuracy to 0.0233%. Further growth of accuracy is negligible since almost all elements of the mesh have less absolute error than the current mean absolute error δ_m in an element (see the last paragraph of Section 3.2) and are not subjected to subdivision.

Data for the force F_m in the fourth column of Table I exhibit rapid monotone convergence to the final value. This value coincides exactly, to three decimal places, with the analogous value in [8] (see Table II) and is in accordance within several tenths of a percent with the corresponding results of [6] and [9]. The magnitude of the force F_m in [8] is probably most accurate at present due to the features of the numerical procedure and taking into account the specific symmetry of the problem. A high prescribed level of accuracy (0.05%), excellent convergence, and accord with the earlier literature data, especially [8], testify to the high quality of the result obtained for F_m.

Convergence of the force F_s in the third column of Table I is worse than that of F_m but is still rather good: values of F_s at the last stages of solution differ from each other within several tenths of a percent. The difference between values of F_s and F_m can also serve as an additional accuracy measure. This difference for the final values of F_s and F_m amounts to 0.19% of F_m. The accordance of F_s with the known literature data in Table II is also within several tenths of a percent.

There are at least two reasons for the accuracy of F_s to be lower than that of F_m. One was mentioned at the end of Section 2. It is that different parts of the spherical surface contribute to the force F_s with opposite signs so that the net value is a sum of pieces which cancel to a considerable degree. The other reason is more significant: the quality of the solution and its gradient near the surface of the particle is lower than that at the other regions of the domain due to the large magnitudes of the gradient. The force F_m does not suffer from this drawback since the gradient, and hence the error, of the solution on the midplane is small. The situation may possibly be improved by employing a more perfect gradient recovery technique, such as superconvergent patch recovery (SPR) [16], and using the recovered gradient for calculations.

The fifth and sixth columns of Table I contain the number of segments and the length of the biggest segment of the broken line representing the circular boundary. The initial geometric shape of the boundary (without respect to the accuracy of solution) is created at the stage of initial mesh generation. Then the representation of the boundary is refined in accordance with the accuracy requirements during the adaptive solution process. The data in Table I demonstrate gradual refinement of the representation throughout the process.

The numerical results presented indicate that the proposed mesh enrichment procedure can maintain the high accuracy level. The procedure demonstrates an ability to gradually improve the quality of the solution and the geometry of the problem. Since the method does not exploit any specific features of the problem, such as specific symmetry, it is expected to be useful for problems with more complex geometries and boundary conditions.

ACKNOWLEDGMENT

The author thanks Professor W. Richard Bowen for the paper [9].

REFERENCES

1. E. J. W. Verwey and J. Th. G. Overbeek, *Theory of the Stability of Lyophobic Colloids* (Elsevier, New York, 1948).

2. W. B. Russel, D. A. Saville, and W. R. Schowalter, *Colloidal Dispersions* (Cambridge Univ. Press, Cambridge, UK, 1989).
3. A. E. Larsen and D. G. Grier, *Nature* **385**, 230 (1997).
4. N. E. Hoskin and S. Levine, *Philos. Trans. R. Soc. London A* **248**, 433 (1056); 449 (1956).
5. L. N. McCartney and S. Levine, *J. Colloid Interface Sci.* **30**, 345 (1969).
6. J. E. Ledbetter, T. L. Croxton, and D. A. McQuarrie, *Can. J. Chem.* **59**, 1860 (1981).
7. B. K. C. Chan and D. Y. C. Chan, *J. Colloid Interface Sci.* **92**, 281 (1983).
8. S. L. Carnie, D. Y. C. Chan, and J. Stankovich, *J. Colloid Interface Sci.* **165**, 116 (1994).
9. W. R. Bowen and A. O. Sharif, *J. Colloid Interface Sci.* **187**, 363 (1997).
10. I. E. Tamm, *Foundations of the Theory of Electricity* (in Russian) (Nauka, Moscow, 1989).
11. O. C. Zienkiewicz and K. Morgan, *Finite Elements and Approximation* (Wiley–Interscience, New York, 1983).
12. J. E. Dennis, Jr. and R. B. Schnabel, *Numerical Methods for Unconstrained Optimization and Nonlinear Equations* (Prentice-Hall, Englewood Cliffs, NJ, 1983).
13. P. E. Dyshlovenko and V. S. Loginov, Srednevolzhskoe (Central Volga Region) Math. Society, Saransk, Preprint 27, 2000 (in Russian).
14. O. C. Zienkiewicz and J. Z. Zhu, *Int. J. Numer. Meth. Eng.* **24**, 337 (1987).
15. B. N. Delaunay, *Bull. Acad. Sci. USSR* **6**, 793 (1934).
16. O. C. Zienkiewicz and J. Z. Zhu, *Int. J. Numer. Meth. Eng.* **33**, 1331 (1992).